Available online at www.sciencedirect.com

ScienceDirect

Procedia Manufacturing 26 (2018) 587–594

Procedia MANUFACTURING

www.elsevier.com/locate/procedia

46th SME North American Manufacturing Research Conference, NAMRC 46, Texas, USA

Experimental Study of Material Removal at Nanoscale

Rapeepan Promyoo[a,b], Hazim El-Mounayri[a,b,*], Mangilal Agarwal[a,b]

[a]*Department of Mechanical and Energy Engineering, Indiana University Purdue University Indianapolis, Indianapolis, IN, 46202, USA*
[b]*Integrated Nanosystems Development Institute,Indiana University Purdue University Indianapolis, Indianapolis, IN, 46202, USA*

Abstract

In order to develop nano-machining into a viable and efficient process, there is a need to achieve a better understand the relation between process parameters (such as feed, speed, and depth of cut) and resulting geometry. In this study, a comprehensive experimental parametric study was conducted to produce a database that is used to select proper machining conditions for guiding the fabrication of precise nano-geometries. The parametric studies conducted using AFM nanosize tips showed the following: normal forces for both nano-indentation and nano-scratching increase as the depth of cut increases. The indentation depth increases with tip speed, but the depth of scratch decrease with increasing tip speed. The width and depth of scratched groove also depend on the scratch angle. The recommended scratch angle is at 90°. The surface roughness increases with step over, especially when the step over is larger than the tip radius. The depth of cut also increases as the step over decreases.

Peer-review under responsibility of the scientific committee of the 46th SME North American Manufacturing Research Conference.

Keywords: Nanomachining; Nanomanufacturing; AFM; Material Removal.

1. Introduction

Tip-based nanomachining generally involves nanoindentation and nanoscratching, which have been commonly used in the characterization of surfaces or small-scale materials [1]. In particular, AFM tips have also been used as cutting tools for surface modification. Nanochannels, nanoslots, and complex nanopatterns can be fabricated by directly scratching the substrate [2]. AFM-based nanomachining is a promising process and is considered a potential manufacturing tool for operations such as machining, patterning, and assembling with *in situ* metrology and visualization [3]. It also has the ability to perform *in situ* repair/re-manufacturing of the position, size, shape, and orientation of single nanostructures. These AFM-based mechanical indentation and scratching techniques have been successfully applied to produce complex geometries and high aspect-ratio 3D nano-objects on both flat and curved surfaces [4]. AFM-based nanomachining is capable of fabricating complex structures. Advances in materials, pattern transfer processes, and cost reductions of AFM equipment have allowed these methods to become a viable but not yet scalable method for many nanoscale devices [5]. Process throughput however is low due to limited removal speed, tip-surface approach, contact detection, desired force profile, and tool wear. Parallel fabrication using multiple AFM tip arrays has been reported [6,7]. However, parallel fabrication currently does not allow precise control over size, shape, position, or orientation of individual structures. A fundamental understanding of substrate deformations/separations and the tip is needed to achieve controllable nanomanufacturing. Attempts have been made to study the correlation between machining parameters, machined geometry, and surface properties for better control of AFM-based nanomachining processes. AFM has been used as a tool for surface modifications since the late 90s. Konikar et

* Corresponding author. Tel.: +1-317-278-3320 ; fax: +1-317-274-9744.
E-mail address: helmouna@iupui.edu

2351-9789
Peer-review under responsibility of the scientific committee of the 46th SME North American Manufacturing Research Conference.
10.1016/j.promfg.2018.07.069

al. [8] machined surface of single-crystal silicon using AFM. They found that the mechanisms of material removal at micro/nanoscale are different from those at the macroscale. Ichida et al. [9] performed nanomachining experiments on silicon surfaces using an AFM integrated with a two-axis capacitive force/displacement transducer to investigate the effects of applied forces and tip shapes on the scratching characteristics. They concluded that when the applied normal forces is higher than 50 μN, the tip shape begins to affect the processing characteristics. Sun et al. [10] conducted AFM experiments on single crystal copper using a diamond tip to analyze machining parameters, such as velocity, applied force, and feed rate. They were able to create microstructures using the optimized parameters. Yan et al. [11] proposed a calibration method to measure force components in AFM scratching test. They also conducted the AFM scratching test on sapphire substrate using a diamond tip to measure friction coefficient. Wang et al. [12] conducted AFM-based nanomachining on silicon oxide surfaces using a diamond indenter probe to investigate the effects of normal force and cutting velocity on cutting depth and friction force. They concluded that the nanochannel depth is independent of cutting velocity, but increases linearly with the normal force. Geng et al. [13] conducted nanoscratching experiments using a pyramidal diamond tip on aluminum alloy surface. They investigated the effects of cantilever deformation and tip-sample contact area during scratching in different directions. More recently, Zhang et al. [14] conducted nanoscratching experiments on 6H-SiC by using Berkovich indenter to study the relationship between the applied normal load and the machined depth. These efforts include experiments on a few types of materials to investigate the effects of parameters such as applied load, scratching speed, feed rate, scratching direction, tip geometry, tip angle, tip radius, and number of scratching cycles. These parameters which also depend on material properties and crystal orientation of the substrate, affect the depth, width, chip formation, and surface roughness of the machined surface.

In this paper, AFM-based nanomachining (nanoindentation/nanoscratching) experiments were conducted to investigate the effects of applied force, indent speed, scratch length, scratch speed, and scratch angle on different types of material. The machined geometries, i.e. width and depth, were measured and compared.

2. Methodology

Atomic force microscope (AFM) is one type of scanning probe microscopes used for studying surface properties at atomic- and up to micro- scale. AFM can be used to study all materials regardless of opaqueness or conductivity. Typically, AFM is operated in air, but can be used in other environments, such as liquid or vacuum. AFM provides resolution at the nanometer (lateral) and angstrom (vertical) scales. Because of its resolution, flexibility and versatility, AFM has become more widely used in research and development. In addition to its powerful imaging and measuring capabilities, its recent improvements in speed, sensitivity, and ease of use have made AFM a promising tool for nanoscale fabrication. In AFM-based nanomachining, the AFM tip is used as a tool for material removal or surface modification of nanoscale materials. In this study, a Veeco Bioscope AFM, shown in Figure 1 was used to conduct AFM-based TBN experiments. Two types of indenter tips (Bruker AFM probes) , diamond and silicon, were used. The indenter tips have three-sided pyramid shapes with a radius of curvature 40 nm and height of 50 μm. The front, back, and side angles are 55°, 35°, and 51°, respectively. A diamond probe with a spring constant, k, of 243 N/m and a silicon probe with a spring constant of 200 N/m were used in the experiments.

Fig. 1. Veeco Bioscope AFM.

After engaging on sample surface in Tapping mode and locating area of interest, nanoindentation/nanoscratching can be performed. The input parameters investigated in this work are trigger threshold (applied force) and scan rate (speed) for nanoindentation, trigger threshold (applied force), scan rate (speed), scratch rate, scratch length, and scratch angle for nano-

scratching. The following is a description of the investigated input parameters.

1) Trigger threshold

Before making an indentation or scratch, the applied force must be set. This can be done by setting the Trigger threshold parameter. The Trigger threshold is a measure of the force applied to the sample during indentation/scratching. It is the cantilever deflection, specified in volts, at which the controller stop pushing the tip into the surface and lifted up away from the sample to remove the load, if indenting, or the tip is moved laterally in a specified direction, if scratching.

2) Scan rate

The scan rate is the speed at which the cantilever is loaded and unloaded during indentation and scratching. The unit of scan rate is Hertz (Hz). If the scan rate is set on 1 Hz, it will take 1 second to make an indentation. Even though the scan rate is limited to a range of 0.01 Hz to 260 Hz for Veeco Bioscope system, values from 0.5 Hz to 10 Hz are typically used for indentation.

3) Scratch rate

The scratch rate is defined as the speed of the tip during scratching in Hz. When selecting the Scratch rate, both scratch force and length must be considered. Suggested Scratch rates are from 0.5 to 5 Hz.

4) Scratch length

The scratch length (in microns or nanometers) is limited by the maximum Scan size of the AFM scanner. A typical value of the Scratch length is 1-3 μm.

5) Scratch angle

The Scratch angle at which the scratch is conducted is defined within the X Y plane. This angle is measured in degrees relative to the conventional positive X-axis (see Figure 2). A zero rotation results in a scratch made along the X-axis from left-to-right. A 90° rotation results in a scratch along the y-axis beginning at the bottom. A 180° rotation results in a scratch made along the X-axis, from right-to-left.

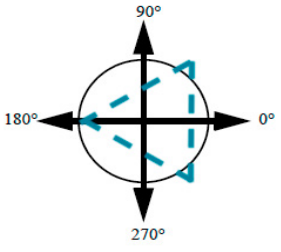

Fig. 2. Scratch angle in Veeco Bioscope AFM.

Tables 1 and 2 summaries the experimental setup for nanoindentation and nanoscratching, respectively.

Table 1. Experimental setup for nanoindentation.

Workpiece material	Gold, Copper, Aluminum, Silicon
Indenter tip material	Diamond, Silicon
Trigger threshold	0.5 - 5 V
Scan rate	1 - 7 Hz

Table 2. Experimental setup for nanoscratching.

Workpiece material	Gold, Copper, Aluminum, Silicon
Indenter tip material	Diamond, Silicon
Trigger threshold	0.5 - 5 V
Scan rate	1 - 7 Hz
Scratch length	1 - 3 μm
Scratch rate	1 - 7 Hz
Scratch angle	$0°, 90°, 180°, 270°$

3. Results and Discussion

AFM-based nanomachining (nanoindentation/nanoscratching) experiments were conducted to investigate the effects of applied force, indent speed, scratch length, scratch speed, and scratch angle on different types of material. The machined geometries, i.e. width and depth, were measured and compared.

3.1. Nanoindentation

Figure 3 shows the AFM image (a) and cross-sectional profile (b) of nanoindentation of gold with diamond tip for different applied forces. The applied force (Trigger threshold) are 1, 2, 3, 4, and 5 Volts increasing from right to left in figure 3(a). The AFM nanoindentation experiments were also conducted on other materials including silicon, copper and aluminum. Each experiment was repeated 5 times (5 rows shown in figure 3(a)) and the average value of depth at different applied force were obtained as shown in figure 4. It can be observed that the indentation depth increases with applied force (Trigger threshold). For the same applied force, aluminum has the highest indentation depth, while silicon has the lowest depth.

Similar AFM nanoindentation experiments were conducted with the use of silicon tip for the case of gold, aluminum, and copper workpiece material. Figure 5 shows the AFM image (a) and cross-sectional profile (b) of nanoindentation of gold with silicon tip for different applied forces. The variation in average value of depth as a function of applied force for different types of material is shown in Figure 6. The indentation depth also increases with applied force. However, the depths obtained from indentation with silicon tip are approximately 4 times lower than those with diamond tip.

The AFM nanoindentation experiments were also conducted to investigate the effect of tip speed (scan

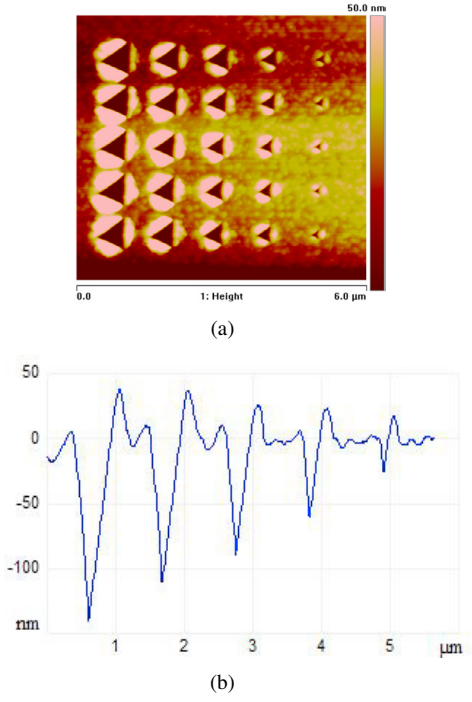

Fig. 3. AFM image (a) and cross-sectional profiles (b) of nanoindentation of gold with diamond tip conducted at different applied forces.

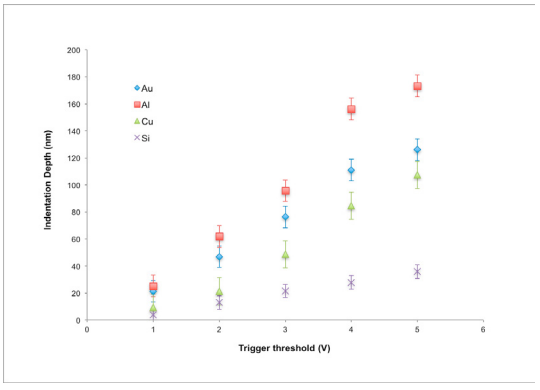

Fig. 4. Indentation depth at different applied forces with diamond tip for different materials.

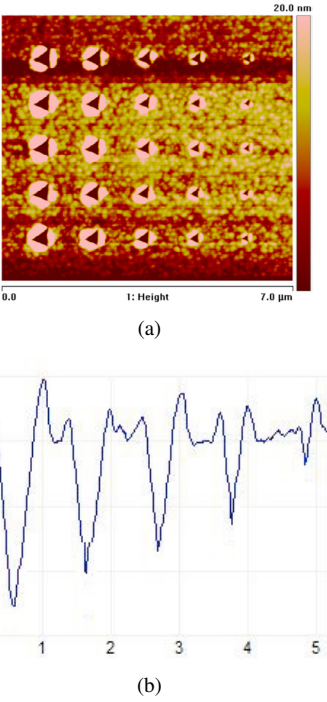

Fig. 5. AFM image (a) and cross-sectional profiles (b) of nanoindentation of gold with silicon tip conducted at different applied forces.

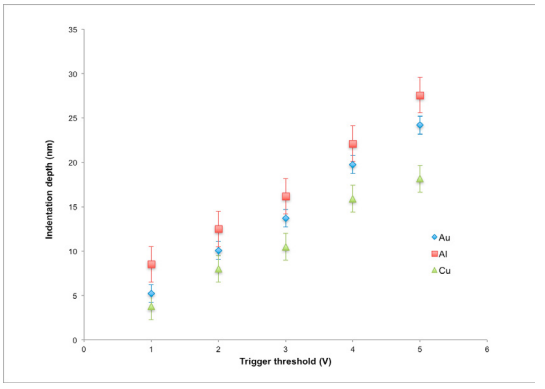

Fig. 6. Indentation depth at different applied forces with silicon tip for different materials.

rate). Figure 7 shows the AFM image (a) and cross-sectional profile (b) of AFM nanoindentation of gold with diamond tip at different tip speeds. The Trigger threshold was kept constant at 3 Volts. The scan rates are 1, 3.016, 4.96, 6.975, and 8.929 Hz from right to left columns. It can be seen from figure 7(b) that the indentation depth increases as the scan rate increases. Figure 8 shows plot of indentation depth at different tip speeds for gold (Au), aluminum (Al), copper (Cu) and silicon (Si). Figure 9 shows the variation in indentation depth at different applied forces and tip speeds for gold with diamond tip.

3.2. Nanoscratching

AFM nanoscratching experiments were performed on different types of material including gold, silicon, copper, and aluminum. Diamond and silicon tips were used for the case of gold, copper, and aluminum workpiece materials. Only diamond tip was used for the case of silicon workpiece material. Figure 10 show

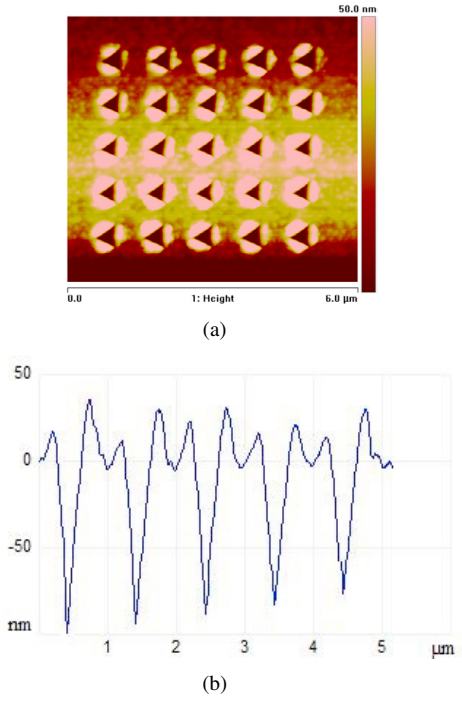

Fig. 7. AFM image (a) and cross-sectional profiles (b) of nanoindentation of gold with diamond tip conducted at different speeds.

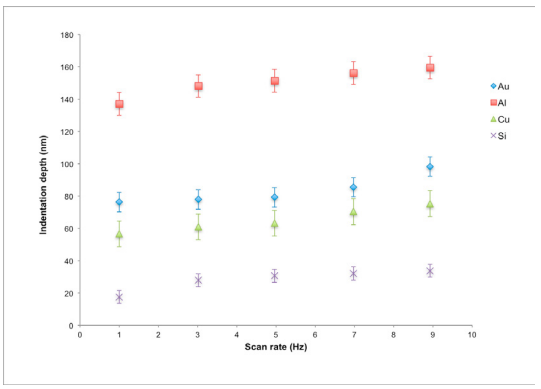

Fig. 8. Indentation depth at different tip speeds for different materials with diamond tip.

AFM image (a) and cross-sectional profiles (b) of nanoscratching of gold with diamond tip at different Trigger threshold. The Trigger threshold of 1, 2, 3, 4, 5 Volts were used in the experiments. The Trigger threshold correspond to the applied force of 48.75, 97.50, 146.25, 195.00, 243.75 μN, respectively. The direction of scratch was at scratch angle of 90° and the scratch rate of 1 Hz was used. The scratch length was 4 μm. The average value of groove depth and width for different types of material at different applied forces are

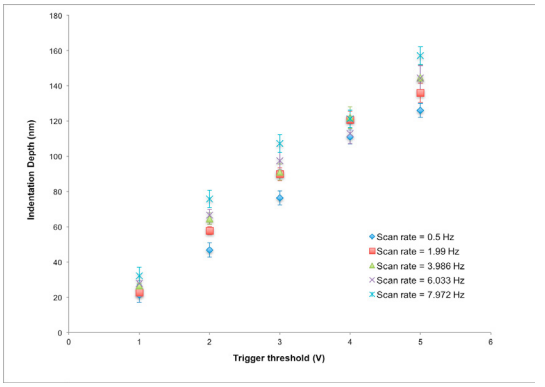

Fig. 9. Indentation depth at different applied forces and tip speeds (scan rates) for gold with diamond tip.

shown in Figure 11 for diamond tip and Figure 12 for silicon tip.

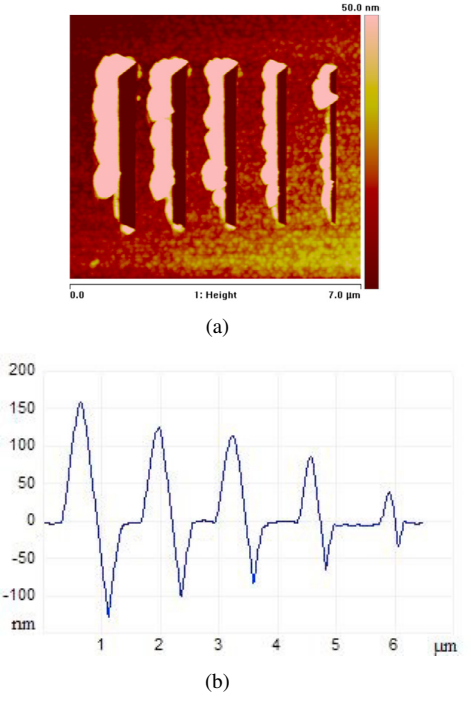

Fig. 10. AFM image (a) and cross-sectional profiles (b) of nanoscratching of gold with diamond tip at different applied forces.

The effect of scratch rate was investigated. The scratch rate used in the nanoscratching experiments are 1.001, 2.94, 5.07, 6.98, and 9.30 Hz. The direction of scratch was at scratch angle of 90° and the trigger threshold of 1 Volt was used. The scratch length was 4 μm. Figure 13 shows AFM image and cross-sectional profile of nanoscratching of gold with diamond tip at different scratch rate. Each experiment was repeated 5

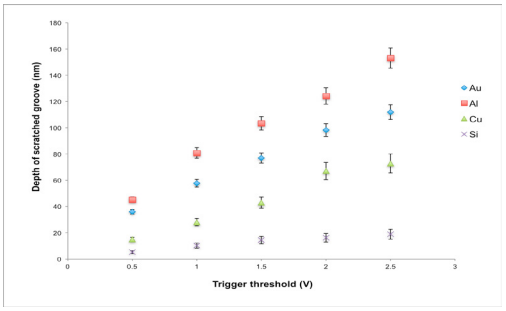

(a)

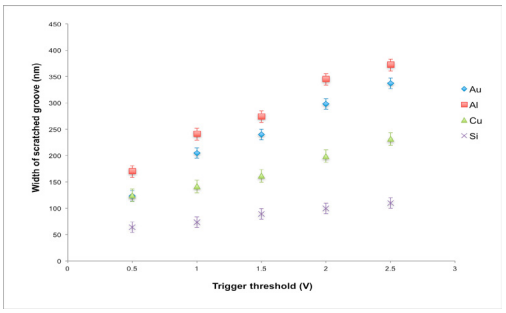

(b)

Fig. 11. Depth (a) and width (b) of scratching groove for different types of material using diamond tip as a function of applied forces.

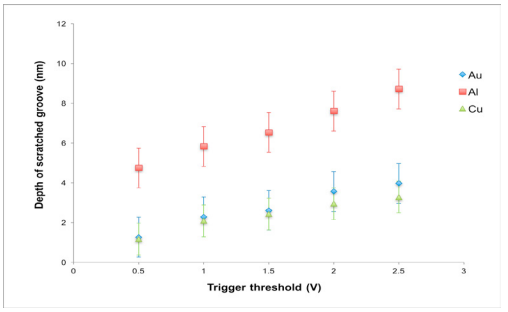

(a)

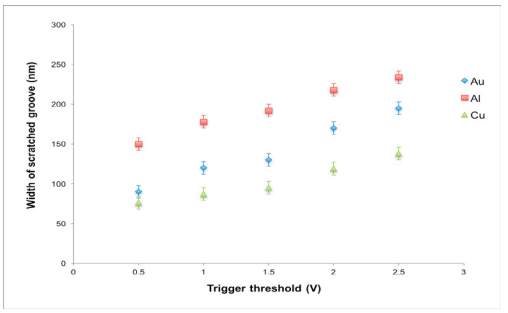

(b)

Fig. 12. Depth (a) and width (b) of scratching groove for different types of material using silicon tip as a function of applied forces.

times and the average values of depth and width of the groove were obtained as shown in figure 14 for different types of material.

The AFM nanoscratching was also conducted to study the effect of scratching direction. The scratch angles used in the experiments were $0°, 90°, 180°, 270°$. Figure 15 shows AFM images of nanoscratching of gold with diamond tip at different scratch angle. The depth and width of the scratching groove are shown in Figure 16.

In addition, the effect of step over (feed) was investigated. 3 μm $\times$ 3 μm square area were fabricated on gold material using different step overs between 10 - 80 nm. The applied force, scan rate, and scratch rate were kept constant. The tip radius is 40 nm. Figures 17 and 18 show the AFM image and cross-sectional profile of the two squares created with the step overs of 10 nm (right) and 20 nm (left). The surface roughness of the machined surface is measured and shown in Table 3. The surface roughness before machining is 1.57 nm. It can be observed from Table 3 that the surface roughness increases with step over. The surface roughness is even more higher when the step over is greater than 40 nm.

Table 3. Surface roughness of the machined surface.

Step over (nm)	Surface roughness (nm)
10	4.38
20	4.81
30	5.49
40	5.77
50	9.53
60	10.21
70	10.98
80	11.42

4. Conclusion

In this work, tip-based nanomachining was experimentally studied by conducting the most comprehensive parametric study. Unique insights into the effect of different input parameters on the process outcome was gained. It was found that the normal force increases with the increase in depth of cut. This was true for both nano-indentation and nano-scratching. The indentation depth increases with tip speed, but the depth of scratch decrease with increasing tip speed. The width and depth of scratched groove also depend on the scratch angle. The surface roughness increases with step over, especially when the step over is larger than the tip radius. The depth of cut also increases as the step over de-

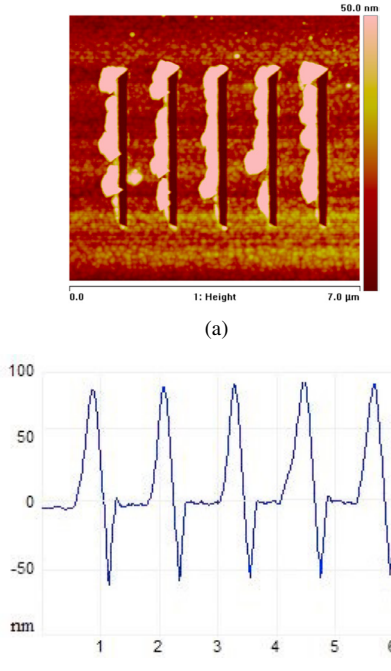

Fig. 13. AFM image (a) and cross-sectional profiles (b) of nano-scratching of gold with diamond tip at different scratch speeds.

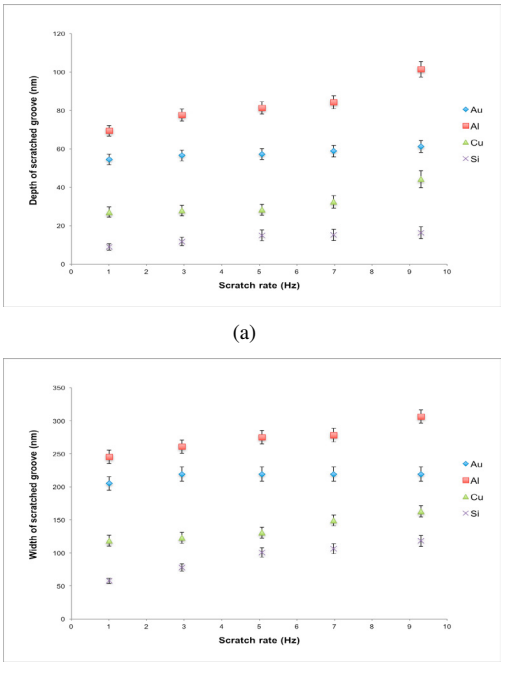

Fig. 14. Depth (a) and width (b) of scratching groove of gold material with diamond tip as a function of scratch speeds.

creases. The resulting database can be used to select proper machining conditions for guiding the fabrication of precise nano-geometries. Future work will extend to different substrate materials, tip shapes, and tip material.

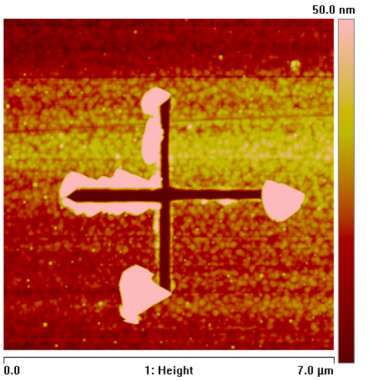

Fig. 15. AFM images of scratching groove at different scratch angles.

References

[1] A. Fischer-Cripps, Nanoindentation, Springer, New York, 2002.
[2] X. Li, P. Nardi, C. Baek, J. Kim, Y. Kim, Journal of Micromechanics and Microengineering 15 (2005) 551–556.
[3] A. Malshe, K. Rajurkar, K. Virwani, C. Taylor, D. Bourell, G. Levy, M. Sundaram, J. McGeough, V. Kalyanasundaram, A. Samant, CIRP Annals - Manufacturing Technology 59 (2010) 628–651.
[4] Y. Yan, T. Sun, X. Zhao, Z. Hu, S. Dong, Journal of Micromechanics and Microengineering 18 (2008) 035002.
[5] S. Diegoli, C. Hamlett, S. Leigh, P. Mendes, J. Preece, Proceedings of the Institution of Mechanical Engineers, Part G: Journal of Aerospace Engineering 221 (2007) 589–629.
[6] S. Minne, G. Yaralioglu, S. Manalis, J. Adams, J. Zesch, A. Atalar, C. Quate, Applied Physics Letters 72 (1998) 2340–2342.
[7] Y. Geng, Y. Yan, X. Zhao, Z. Hu, Y. Liang, T. Sun, S. Dong, Applied Surface Science 266 (2013) 386–394.
[8] V. Koinkar, B. Bhushan, Journal of Materials Research 12 (1997) 3219–3224.
[9] Y. Ichida, Y. Morimoto, R. Sato, M. Murakami, Technical Proceedings of the 2003 Nanotechnology Conference and Trade Show 1 (2003) 534–537.
[10] T. Sun, Y. Yan, J. Xia, S. Dong, Y. Liang, K. Cheng, Key Engineering Materials 259–260 (2004) 577–581.
[11] Y. Yan, S. Dong, T. Sun, Ultramicroscopy 105 (2005) 62–71.
[12] Z. Wang, S. Tung, N. Jiao, Z. Dong, in: Nano/Micro Engineered and Molecular Systems (NEMS), 2010 5th IEEE International Conference on, pp. 637–640. doi:10.1109/NEMS.2010.5592486.
[13] Y. Geng, Y. Yan, Y. Xing, Q. Zhang, X. Zhao, Z. Hu, Journal of Vacuum Science & Technology B 31 (2013) 061802.
[14] F. Zhang, B. Meng, Y. Geng, Y. Zhang, Applied Surface Science 368 (2016) 449–455.

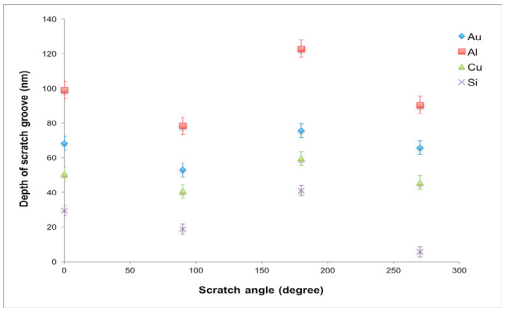

(a)

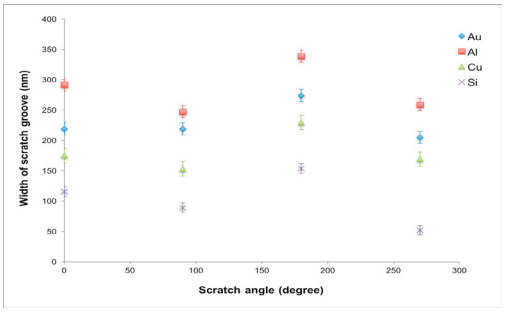

(b)

Fig. 16. Depth (a) and width (b) of scratching groove at different scratch angle.

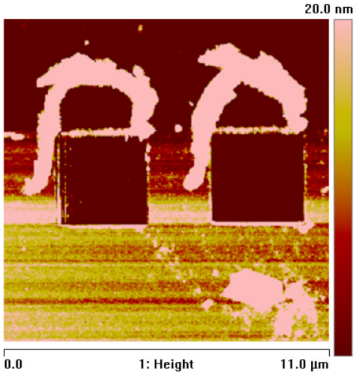

Fig. 17. AFM images of the two nanostructures created with the step overs of 10 nm (right) and 20 nm (left).

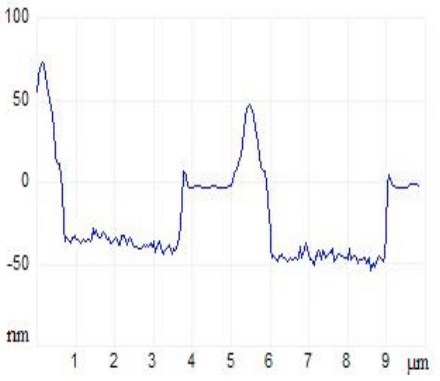

Fig. 18. Cross-sectional profile of the two nanostructures created with the step overs of 10 nm (right) and 20 nm (left).